

Supplementary Information for

RalA controls glucose homeostasis by regulating glucose uptake in brown fat

Yuliya Skorobogatko, Morgan Dragan, Claudia Cordon, Shannon M. Reilly, Chao-Wei Hung, Wenmin Xia, Peng Zhao, Martina Wallace, Denise E. Lackey, Xiao-Wei Chen, Olivia Osborn, Juliane G. Bogner-Strauss, Dan Theodorescu, Christian M. Metallo, Jerrold M. Olefsky, Alan R. Saltiel.

Alan R. Saltiel
Email: asaltiel@ucsd.edu

This PDF file includes:

Supplementary text: supplementary methods
Figs. S1 to S13
Table S1
References for SI reference citations

Supplementary Information Text

Supplementary methods

Reagents

Chemicals used in this study were purchased from MilliporeSigma unless indicated otherwise. Antibody (Ab) against AKT (#9272), S473-AKT (#9272), S308-AKT (#2965), Glut4 clone 1F8 (#2213), and IRAP clone D7C5 XP (#6918) are from Cell Signaling. Other Ab used include RalA (BD Transduction Laboratories, #610222), Glut1 (Novus Biologicals, #NB 110-39113), Na/K ATPase (Abcam, #7671), c-Myc (9E10) (Santa Cruz #sc-40), and F4/80:Biotin (Bio-Rad, #MCA497B). RalGAPB antibody were generated as previously described (7). Secondary Ab for WB: goat anti-rabbit IgG, HRP (ThermoFisher, #31460), goat anti-mouse IgG, HRP (ThermoFisher, #31430), and anti-goat IgG-HRP (Santa Cruz, #sc-2020). Secondary Ab for imaging: Alexa Fluor 594 goat anti-mouse IgG (Invitrogen, #A11032) and Alexa Fluor 488 goat anti-rabbit (Invitrogen, #A11008). RalBP1 agarose for active RalA pulldown was purchased from Millipore (#14-415). Ral inhibitors RBC8 and BQU57 were kindly provided by Dan Theodorescu from University of Colorado, Denver (10). Additionally RBC8 was purchased from Sigma-Aldrich (#SML1295). cDNA encoding 7myc-Glut4-eGFP was a generous gift from Dr. Jonathan Bogan (Yale University); for TIRF imaging 7myc-Glut4-eGFP was subcloned into lentiviral vector PLVX-Puro (Addgene).

3T3-L1 adipocyte culture

3T3-L1 fibroblasts were cultured in 10% neonatal calf serum in DMEM for proliferation and 10% FBS in DMEM for differentiation. Cells were grown to confluence and 2 days later differentiation was induced with 500 μ M 3-isobutyl-1-methylxanthine, 250nM dexamethasone and 1 μ g/ml insulin for 3-4 days followed by insulin-only treatment for 2 days. We routinely used cells within 2 days after completion of the differentiation and only used cultures in which >90% of cells showed adipocyte morphology.

Electroporation

The 3T3-L1 adipocytes were transfected with 200 μ g of Myc7-Glut4-eGFP plasmid by electroporation. In brief, within 2 days after differentiation adipocytes were detached from culture dishes with 0.25% trypsin, washed twice, and resuspended in phosphate-buffered saline (PBS). Approximately 5*10⁶ cells (half of the cells from one p150 dish) were mixed with the plasmid DNA, which was delivered to the cells by electroporation with a Bio-Rad gene pulser II system (Richmond, CA; 0.16kV and 960 μ F). After electroporation, cells were mixed with medium for 10min. before replating. 3-4 days later cells were processed for imaging.

Methanol fixation

Methanol fixation was used to visualize endogenous Glut4 and phospho-AKT473 in 3T3-L1 adipocytes. Media was aspirated, ice-cold methanol was added, and cells were incubated at -20 C° for 10min. The next steps were performed at room temperature. The cells were washed with PBS and permeabilized with 0.1% Triton X-100 in PBS with 10% goat serum for 30min. After washes cell were stained with antibody: primary over

night at 4°C, and secondary for 1h at room temperature; and then mounted on the slides with ProLong Diamond Antifade Mountant (Invitrogen, #P36961).

Formalin fixation

The method was used to fix cells expressing Myc7-Glut4-eGFP to preserve eGFP. The media was aspirated and cells were incubated in 10% formalin, phosphate buffered, 10min at room temperature. Then the cells were incubated with 100mM glycine in PBS for 15min. After washes the cells were processed for staining against Myc epitope without permeabilization.

Confocal microscopy and data acquisition

Cells were imaged with Olympus IX81 inverted confocal microscope with 60x Oil objective (NA = 1.42) and FluoView Viewer Software. Excitation was performed with 488nm and 543nm laser. Quantitation was done using ImageJ software. After background correction, plasma membranes (PM) were manually selected based on phospho-AKT473 staining, and data for Glut4 channel mean intensity was extracted (this is PM-localized Glut4). The cytosolic Glut4 is calculated as a difference between total Glut4 intensity and PM-localized Glut4. For quantitation of Myc7-Glut4-eGFP localization Myc signal, which stained plasma membranes only, was manually selected and divided by total cell eGFP intensity.

TIRG microscopy; processing of images

ImageJ was used to process and quantify images. To calculate corrected total cell fluorescence, raw TIRF images were first processed by rolling ball background subtraction algorithm, available as an ImageJ plug-in (https://imagej.net/Rolling_Ball_Background_Subtraction). Cells were then manually selected and total cell fluorescent (TCF) was measured with ImageJ. Finally, a small region of interest outside of cells was drawn to measure the background intensity and then subtracted from TCF. To measure the intensity of each independent Glut4 cluster, a threshold was calculated using ImageJ after background was corrected by Rolling Ball background subtraction algorithm, described in the previous paragraph. Each cluster was identified and intensity was measured by ImageJ. Movement of Glut4-GFP particles was evaluated by Mosaic particle tracker, available as a plugin of Fiji. To calculate diffusion coefficient, the mean square displacement (MSD) versus the time interval τ plot was generated ($MSD(\tau) = 4D\tau$). The initial slope (D) of the plot is then calculated and determined to be diffusion coefficient (1-3). Particle were tracked for at least 10 frames (5 seconds).

Generation of 3T3-L1 adipocytes stably expressing Myc7-Glut4-eGFP

Production of lentivirus was carried out in 293T cells described previously (4). Briefly, 10 μ g of lentiviral expression vectors (7myc-Glut4-eGFP in PLVX-Puro), 7.5 μ g lentiviral packaging plasmid psPAX2 and 2.5 μ g of VSV-G pMD2.G were mixed with lipofectamine 3000 packaging mix (Invitrogen) and then transfected into 293T cells grown on a 15cm dish. The medium was changed after 18 hours. Viruses were harvested 48h and 72h post-transfection. The viruses were concentrated using 100kDa centrifugal filter units (Millipore). The concentrated infectious media were used to infect 3T3-L1

preadipocytes grown on 10cm dishes in a media containing 8µg/ml of polybrene for at least 24h. GFP-positive cells were collected by flow cytometry.

Generation of RalGAPB knockout mice

Mice with conditional knockout of RalGAPB were derived from ES cell containing allele Ralgapbtm355629(L1L2_Bact_P) (European Mouse Mutant Cell repository), where 3rd exon of *Ralgapb* gene is surrounded by loxP sites. *Ralgapb* fl/fl mice were bred with adiponectin-cre mice to generate adipocyte-specific *Ralgapb* knockout mice. The knockout (fl/fl cre+) and control (fl/fl cre-) mice are litter mates and cage mates.

Diet

Normal chow diet consists of 4.5% fat (5002 Lab Diet). Male mice were fed HFD containing 45% of calories from fat (D12451 Research Diets Inc.) starting at 8 weeks of age for 12–24 weeks.

Digestion of fat pads with collagenase and isolation of Stromal vascular fraction (SVF) Excised WAT was digested in PBS containing 1% BSA and 1mg/ml type II collagenase for 30min at 37°C with gentle agitation. The cell suspension was filtered through a 100µm filter and then centrifuged at 2,000g for 5min to separate floating adipocytes from the SVF pellet.

Primary adipocytes

To generate primary white adipocytes inguinal fat depots were dissected from 2 month old mice. To generate primary brown adipocytes BAT was dissected from 3 to 4 week old mice. SVF fraction was prepared as described above and plated. DMEM/F12 media with 15% FBS, glutamine, and penicillin/streptomycin was used throughout the protocol, except for during differentiation the media with 10% FBS was used. When cells reached 80% confluence they were split 1:6, and then grown to a confluency. 2 days later differentiation cocktail was added (5 µM dexamethazone, 0.5µg/ml insulin, 0.5mM 3-isobutyl-1-methylxanthine, 1 µM troglitazone), on day 4 cells were switched to insulin only cocktail, and were used on day 7 or 8.

Blood chemistry analysis.

Blood glucose was measured by OneTouch Ultra Glucometer. Plasma from mice fasted for 6h was isolated from whole blood collected into heparinized tubes. An insulin ELISA kit (Crystal Chem Inc.) was used to measure insulin concentrations in serum.

Glucose and insulin tolerance tests.

For glucose tolerance tests, after a 6h fast, mice were intraperitoneal (IP) injected with glucose at a dose of 1.5g per kg body weight for lean mice and 1.2g per kg body weight for mice on high fat diet. For insulin tolerance tests, mice were fasted for 3h and then given an IP injection of insulin: 1.2 units per kg body weight for lean mice and 1.5 units per kg body weight for mice on high fat diet. We measured the basal blood glucose level and then performed the measurements at 15, 30, 45, 60, 90, 120 and 180min in tail blood.

Food intake.

The remaining weight of food provided was determined daily for singly housed mice. Daily food consumption was calculated from a 7 day average.

Food withdrawal.

The food was removed in the beginning of the dark cycle. Blood glucose levels were measured as a time course. Simultaneously plasma was collected to measure insulin levels.

Tissue-specific insulin sensitivity.

Tissues were collected 15min after overnight fasted mice were injected with insulin (1 U/kg) via IP. The tissues were frozen in liquid nitrogen, stored at -80°C, then lysed in ICK buffer and processed for WB with phospho-AKT473 antibody.

Western blot analysis.

Tissues were homogenized in ICK buffer: 50mM Tris-HCl, pH 7.4, 150mM NaCl, 10mM MgCl₂, 1mM dithiothreitol (DTT), 1mM phenylmethylsulfonyl fluoride, 10% glycerol, 1% triton X-100, phosphatase inhibitor cocktail 1 and 2 (Roche), and protease inhibitor tablet (Sigma). Homogenates were incubated with rotation at 4°C for 30min. and then centrifuged at 15,000g for 15min. The protein concentration in supernatants was determined using BioRad Protein Assay Reagent. Samples were diluted in SDS sample buffer with 50mM DTT, boiled for 5min., resolved by SDS-PAGE, and transferred to nitrocellulose membranes (Bio-Rad). Individual proteins were detected with the specific antibodies and visualized on film using horseradish peroxidase-conjugated secondary antibodies and Western Lightning Enhanced Chemiluminescence (Perkin Elmer Life Sciences). Bands were quantified with ImageJ.

In vivo tissue-specific glucose uptake

After mice were fasted for 6h, plasma was collected for insulin measurement and 10 μ Ci of deoxy-D-2-[¹⁴C(U)]-glucose (specific activity 250-350mCi (9.25-13.0GBq)/mmol; Perkin Elmer, #NEC720A250UC) was injected via IP. Blood glucose was measured and 20 μ l blood glucose samples were collected at 5, 10, 20, and 30min time points to determine specific activity of the tracer in plasma. At 30min mice were sacrificed, tissues were collected, frozen in liquid nitrogen, and stored at -80°C till processing. Tissues were weighed, homogenized using tissue-tearer in 1ml. of water, and heated to 70°C for 10min. with vigorous shaking. Then the samples were centrifuged for 5min. at 10,000g at room temperature. Deoxy-D-glucose-6-phosphate was purified from supernatant by gravity flow on columns packed with AG 1-X8 resin, acetate form (Bio-Rad, #140-1443). After the supernatants were applied on columns, columns were washed with 5 volumes of water, and then eluted with 5 volumes of 0.2M formic acid/0.5M ammonium acetate buffer. The eluate was used for scintillation counting (5). Disintegration per min. units were converted to nmole of glucose taken up by the tissue (or nmole glucose per gram of tissue) using average specific activity of the tracer in plasma during the experiment. Prior to column chromatography of the supernatants control purifications were performed to determine the volume of the supernatant for each tissue which allows to recover at least 90% of deoxy-D-glucose-6-phosphate. Various volumes of a lysate of a corresponding tissue (initially not containing radioactivity) was spiked with deoxy-D-2-

[H3]-glucose and deoxy-d-glucose, 2-[1-14C] 6-phosphate disodium salt (Americal Radiolabelled Chemicals, #ARC 1319). And efficiency of separation of the two radionucleotides was determined.

Mass spectrometry of plasma membrane fractions

Sample preparation: Protein samples were diluted in TNE (50mM Tris pH 8.0, 100mM NaCl, 1mM EDTA) buffer. RapiGest SF reagent (Waters Corp.) was added to the mix to a final concentration of 0.1% and samples were boiled for 5min. TCEP (Tris (2-carboxyethyl) phosphine) was added to 1mM (final concentration) and the samples were incubated at 37°C for 30min. Subsequently, the samples were carboxymethylated with 0.5mg/ml of iodoacetamide for 30min at 37°C followed by neutralization with 2mM TCEP (final concentration). Proteins samples prepared as above were digested with trypsin (trypsin:protein ratio - 1:50) overnight at 37°C. RapiGest was degraded and removed by treating the samples with 250mM HCl at 37°C for 1h followed by centrifugation at 14,000rpm for 30min at 4°C. The soluble fraction was then added to a new tube and the peptides were extracted and desalted using C18 desalting columns (Thermo Scientific, PI-87782). Peptides were quantified using BCA assay and a total of 1µg of peptides were injected for LC-MS analysis.

LC-MS-MS: Trypsin-digested peptides were analyzed by ultra high pressure liquid chromatography (UPLC) coupled with tandem mass spectroscopy (LC-MS/MS) using nano-spray ionization. The nanospray ionization experiments were performed using a Orbitrap fusion Lumos hybrid mass spectrometer (Thermo) interfaced with nano-scale reversed-phase UPLC (Thermo Dionex UltiMate™ 3000 RSLC nano System) using a 25 cm, 75-micron ID glass capillary packed with 1.7-µm C18 (130) BEHTEM beads (Waters corporation). Peptides were eluted from the C18 column into the mass spectrometer using a linear gradient (5–80%) of ACN (Acetonitrile) at a flow rate of 375µl/min for 1h. The buffers used to create the ACN gradient were: Buffer A (98% H₂O, 2% ACN, 0.1% formic acid) and Buffer B (100% ACN, 0.1% formic acid). Mass spectrometer parameters are as follows; an MS1 survey scan using the orbitrap detector (mass range (m/z): 400-1500 (using quadrupole isolation), 120000 resolution setting, spray voltage of 2200 V, Ion transfer tube temperature of 275 C, AGC target of 400000, and maximum injection time of 50 ms) was followed by data dependent scans (top speed for most intense ions, with charge state set to only include +2-5 ions, and 5 second exclusion time, while selecting ions with minimal intensities of 50000 at in which the collision event was carried out in the high energy collision cell (HCD Collision Energy of 30%), and the fragment masses were analyzed in the ion trap mass analyzer (With ion trap scan rate of turbo, first mass m/z was 100, AGC Target 5000 and maximum injection time of 35ms). Protein identification and label free quantification was carried out using Peaks Studio 8.0 (Bioinformatics solutions Inc.) (6).

Gene expression analysis

Unless indicated otherwise mice were fasted for 6h before collecting tissues for gene expression analysis. The mouse tissues were rinsed in PBS, frozen in liquid nitrogen, and stored at -80 °C until extraction. Liver, iWAT, eWAT, BAT, or gastrocnemius muscle were homogenized in Trizol Reagent (Life Technologies). RNA was isolated with

PureLink RNA mini kit (Life Technologies). 2 μ g of purified RNA was used for reverse transcription-PCR to generate cDNA using TaqMan[®] One-Step RT-PCR Master Mix (Thermo Fisher) with oligo dT primers for reverse transcription. Real-time PCR amplification of the complementary DNA was performed on samples in triplicate with Power SYBR Green PCR Master Mix (Applied Biosystems) using the Applied Biosystems 7900HT Fast real-time PCR System. ArBP and Cyclophilin A were used as the internal controls for normalization after screening of several candidate genes; their expression was not substantially affected by experimental conditions. The sequences of all primers used in this study are listed in [Supplementary Table 1](#). The data were quantified using an internal standard curve.

Histochemistry.

Tissues were fixed in phosphate-buffered formalin for 1 (liver) or 7 days (fat depots), and then stored in 70% ethanol. The Histology Core at University of Michigan School of Dentistry or Histology and Immunohistochemistry Core at Moores Cancer Center performed histology. For cell size quantitation H&E stained slides were imaged in the red fluorescens channel. Automatic particle counting was done on inverted images using ImageJ software.

Hyperinsulinemic-euglycemic clamp

In brief, mice implanted with dual jugular catheters 3 days previously were fasted for 6h, then equilibrated for 90min with tracer (5.0 μ Ci h^{-1} , 0.12ml h^{-1} d-[3-3H]glucose; NEN Life Science Products). A basal blood sample was then drawn via tail vein to calculate basal glucose uptake. The insulin (8 mU kg^{-1} min^{-1} at 2 μ l min^{-1} ; Novo Nordisk) plus tracer (5.0 μ Ci h^{-1}) and glucose (50% dextrose at variable rate; Abbott) infusions were initiated simultaneously, with the glucose flow rate adjusted to reach a steady-state blood glucose concentration (\sim 120min). Steady state was confirmed by stable plasma tracer counts during the final 30min of clamp. Blood was taken at 110 and 120min for the determination of tracer-specific activity. At steady state, the rate of glucose disappearance or the total glucose disposal rate is equal to the sum of the rate of endogenous or hepatic glucose production and the rate of exogenous glucose infusion. The insulin-stimulated glucose disposal rate is equal to the total glucose disposal rate minus the basal glucose turnover rate. For tissue-specific glucose disposal calculations, mice were injected with 10 μ Ci of C-14 deoxy-d-glucose after reaching steady-state blood glucose concentrations. And the procedure was completed as described above for tissue-specific glucose uptake in fasted animals.

Supplementary figures

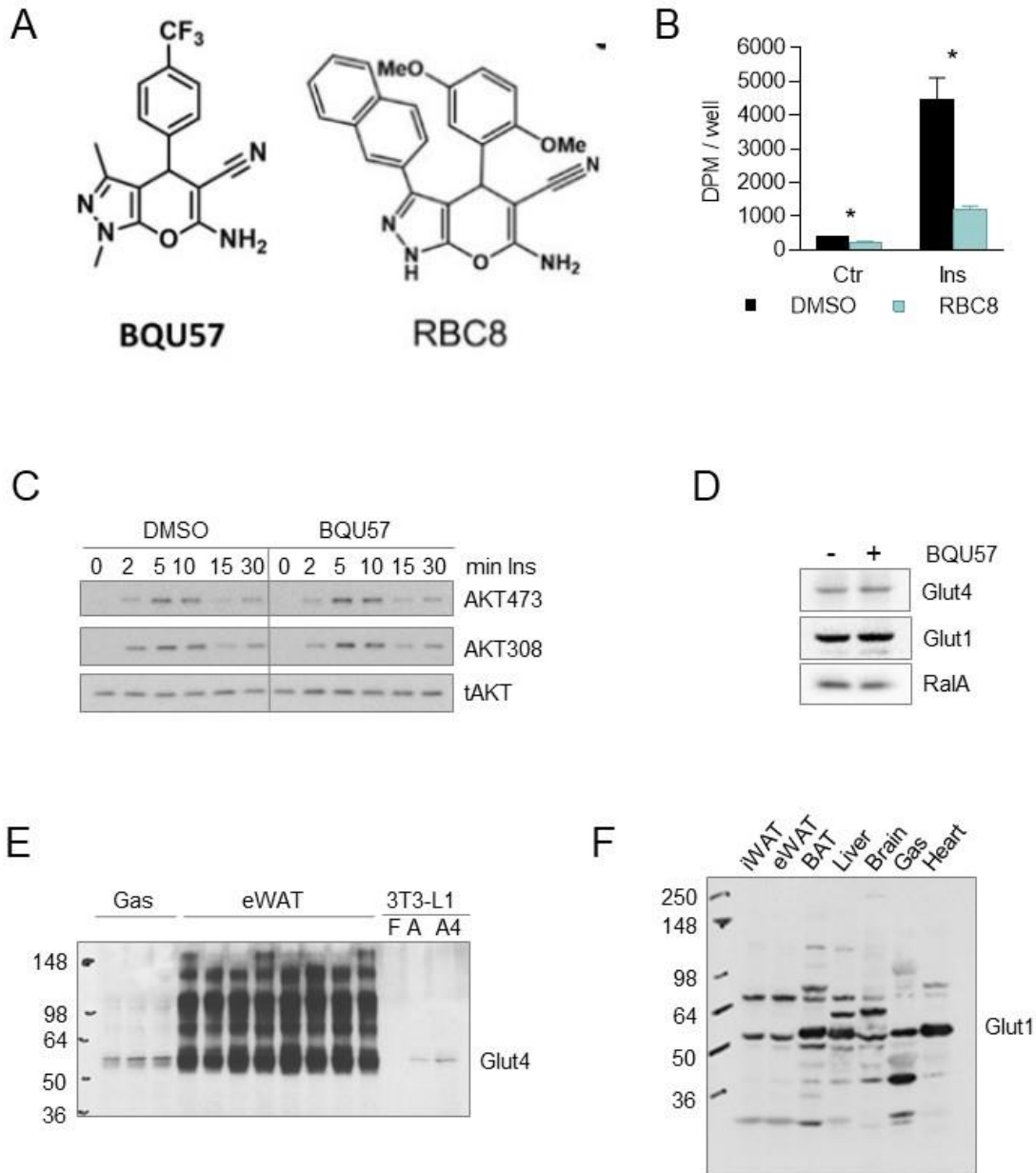


Figure S1. Ral inhibitors in 3T3-L1 adipocytes.

A, Chemical structures of indicated Ral inhibitors. *B*, 2-deoxy-D-glucose uptake in 3T3-L1 adipocytes pretreated RalA inhibitor RBC8 (50uM) for 1 hr. in basal and insulin-stimulated conditions. *C*, *D*, 3T3-L1 adipocytes were pretreated for 1 hr. with 100 uM BQU57, and stimulated with 10 nM insulin for additional 30 min (in the presence of BQU57) and then were processed for WB with indicated Ab. *E*, *F*, Anti-Glut4 Ab (clone F8, Cell Signaling) (*E*) and anti-Glut1 Ab (Novus Biologicals) (*F*) were tested using lysates from indicated mouse tissues, or 3T3-L1 fibroblasts (*F*) and 3T3-L1 adipocytes (*A* and *A4*; lane *A4* contain 4 times more protein than lane *A*).

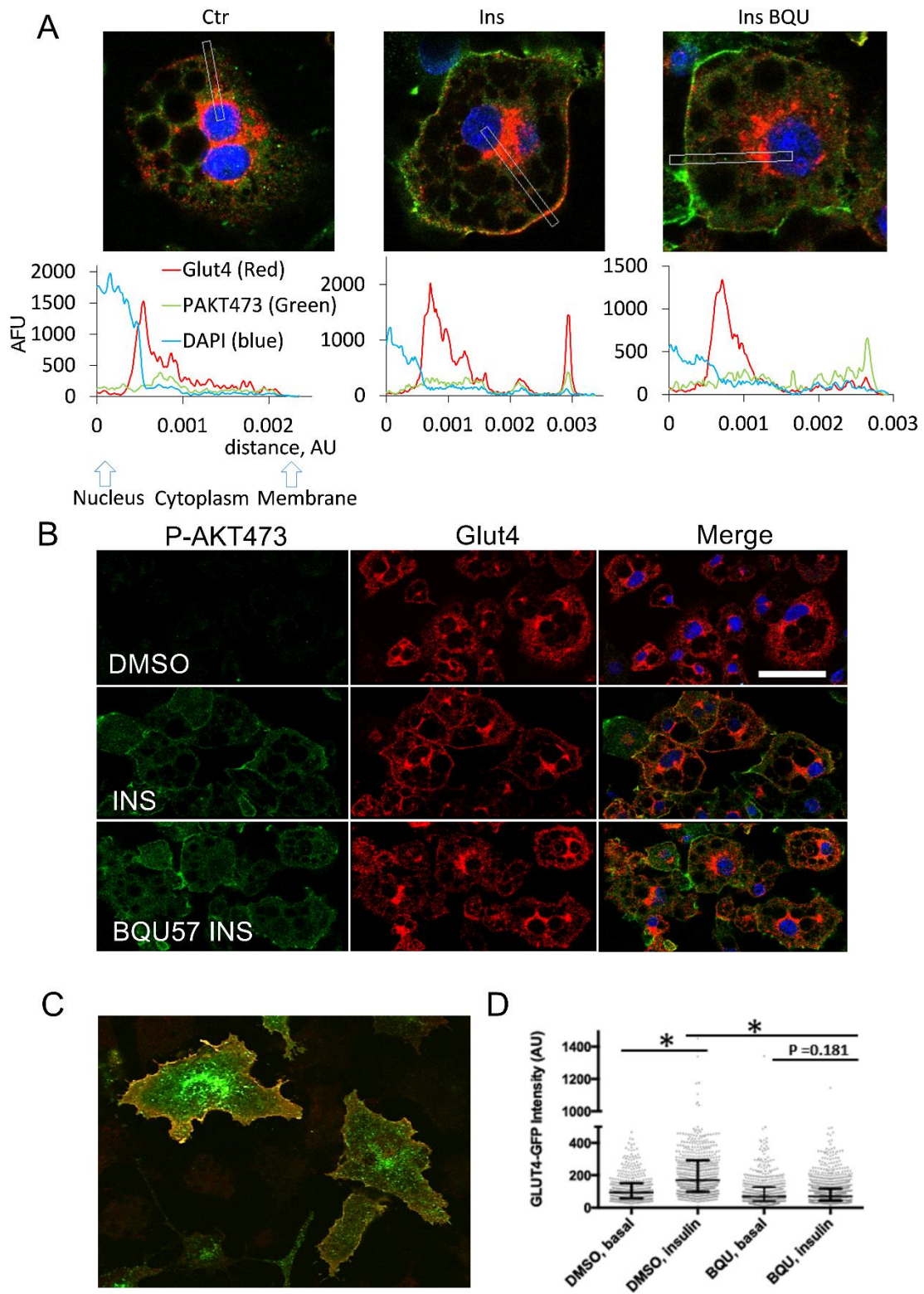


Figure S2. BQU57 inhibits translocation of Glut4 in response to insulin in 3T3-L1 adipocytes.

A, B, Confocal imaging of endogenous Glut4 localization in 3T3-L1 adipocytes in basal, stimulated with 10nM insulin for 30min, and insulin-stimulated after 1 h. pretreatment with 100uM BQU57. Line plot intensity profiles shown below. Red- Glut4, Green – PAKT473, blue – DAPI. *C*, 3T3-L1 adipocyte electroporated with Myc7-Glut4-eGFP, later treated with 10nM insulin for 30 min and stained without permeabilization for Myc tag (red). Data presented in the fig. 1c is generated from the images like that. *D*, Intensities of individual Glut4-eGFP puncta in the TIRF zone. Quantified based on images like in fig. 1 f.

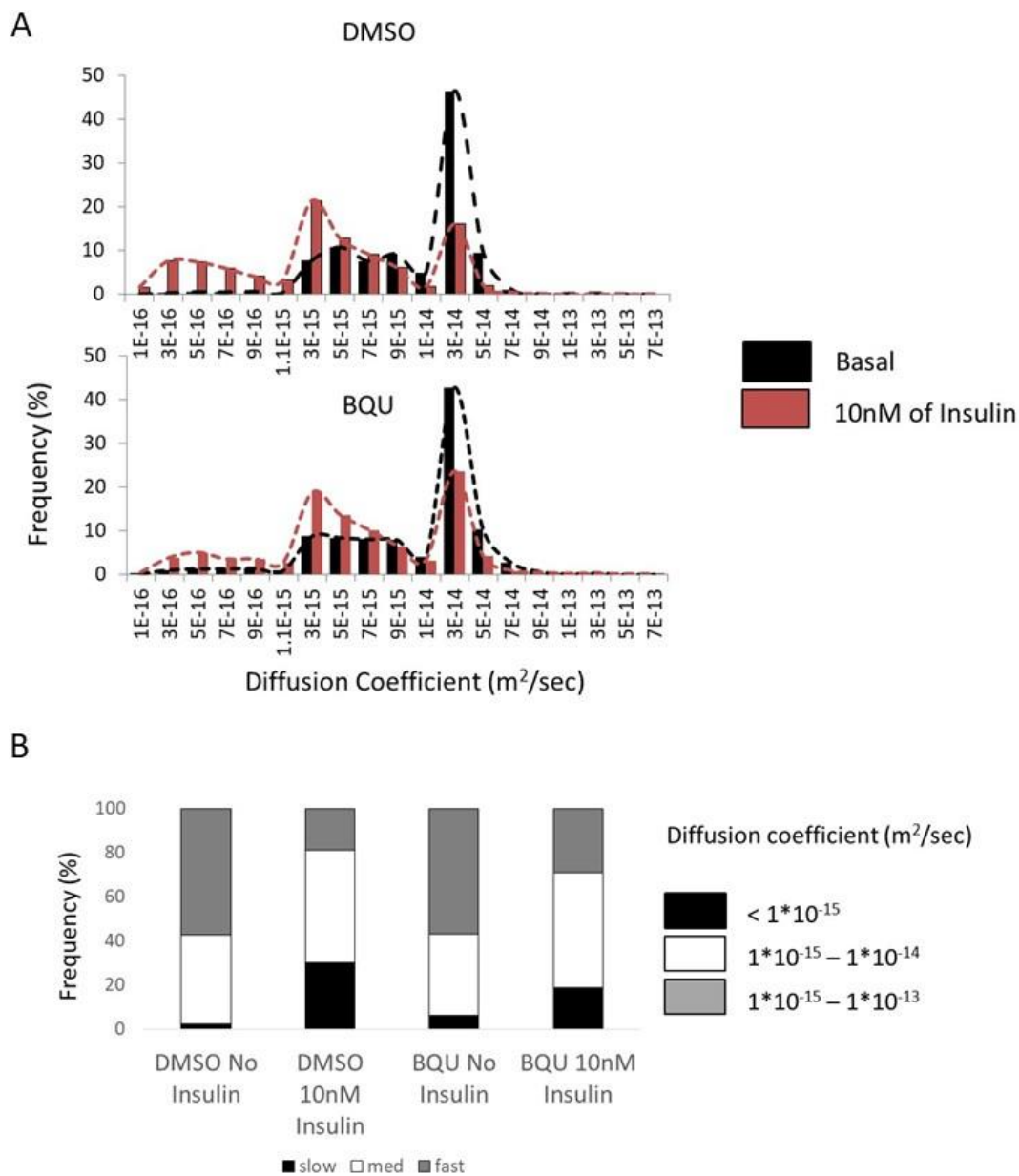


Figure S3. BQU57 inhibits tethering/docking of Glut4 in response to insulin in 3T3-L1 adipocytes.

A, Histograms of the diffusion coefficient of GLUT4 vesicles with or without insulin stimulation. Dash lines indicate the corresponding distribution curves. *B*, Diffusion coefficient was calculated for individual Glut4-eGFP puncta. Based on the calculated values the puncta were split into three groups: slow, medium, and fast moving vesicles. Slow moving vesicles correspond to vesicles preparing for the fusion. The fractional composition of total pool of Glut4-eGFP puncta in the TIRF zone based on the speed of movement under different conditions is shown.

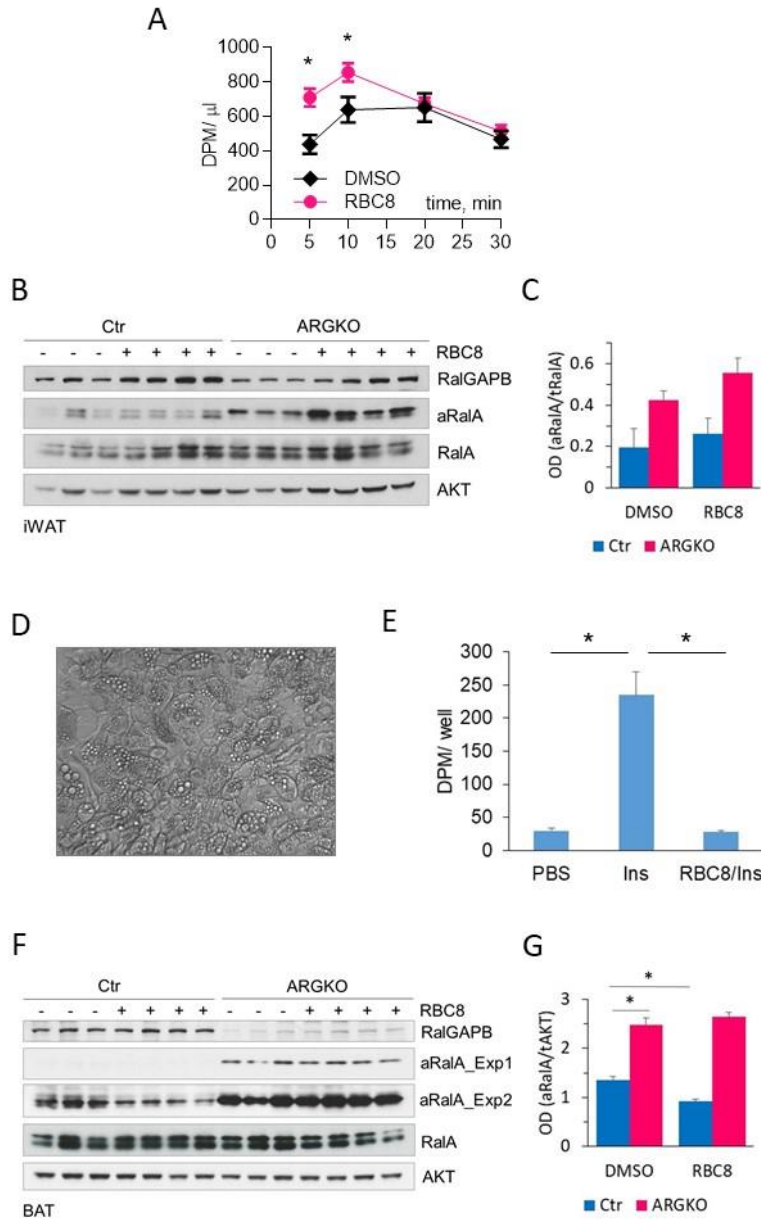


Fig. S4. RBC8 inhibits glucose uptake *in vivo* and *ex vivo*.

A, Glucose tracer decay in plasma. The mice were injected with 50mg/kg RBC8 or DMSO via IP, 40 min later 10uCi of 2-deoxy-D-Glucose [C14] were administered via IP. 8 animals per group were used. Supplementary to fig. 1k. B, WB. RalA activity in iWAT 40 min after *ad libitum* fed mice were injected with RBC8, 50mg/kg. Active RalA pulled with RalPB1 beads. C, Densitometry of images in panel B. D, Phase contrast image of primary brown adipocytes used for glucose uptake experiment in fig. 1 l. E, *De novo* lipogenesis measured in primary adipocytes differentiated from iWAT-derived preadipocytes. The cells were pretreated with 50uM RBC8 or DMSO, and stimulated with 10nM insulin for 30min. F, WB. RalA activity in BAT 40 min after *ad libitum* fed mice were injected with RBC8, 50mg/kg. Active RalA pulled with RalPB1 beads. G, Densitometry of images in panel B.

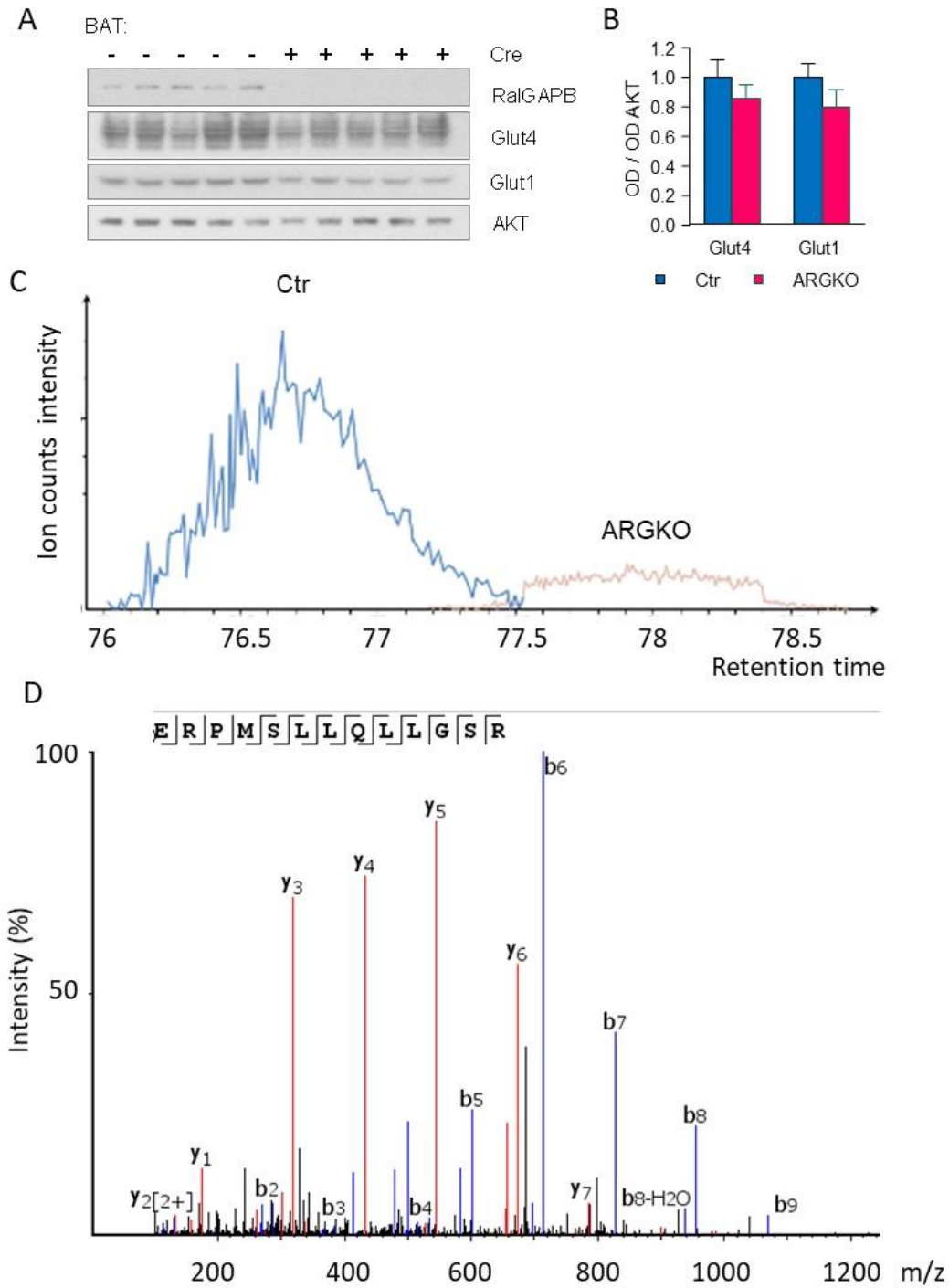


Fig. S6. Plasma membrane Glut4 is increased in the BAT of ARGKO mice.

A, B, WB of lysates from BAT and its densitometry. Tissues were collected after 6hr fast. *C, D*, plasma membrane fraction from BAT was analyzed on LC-MS and quantified using label-free approach. *C*, Ion counts for a Glut4 peptide. *D*, Fragmentation spectra for the peptide.

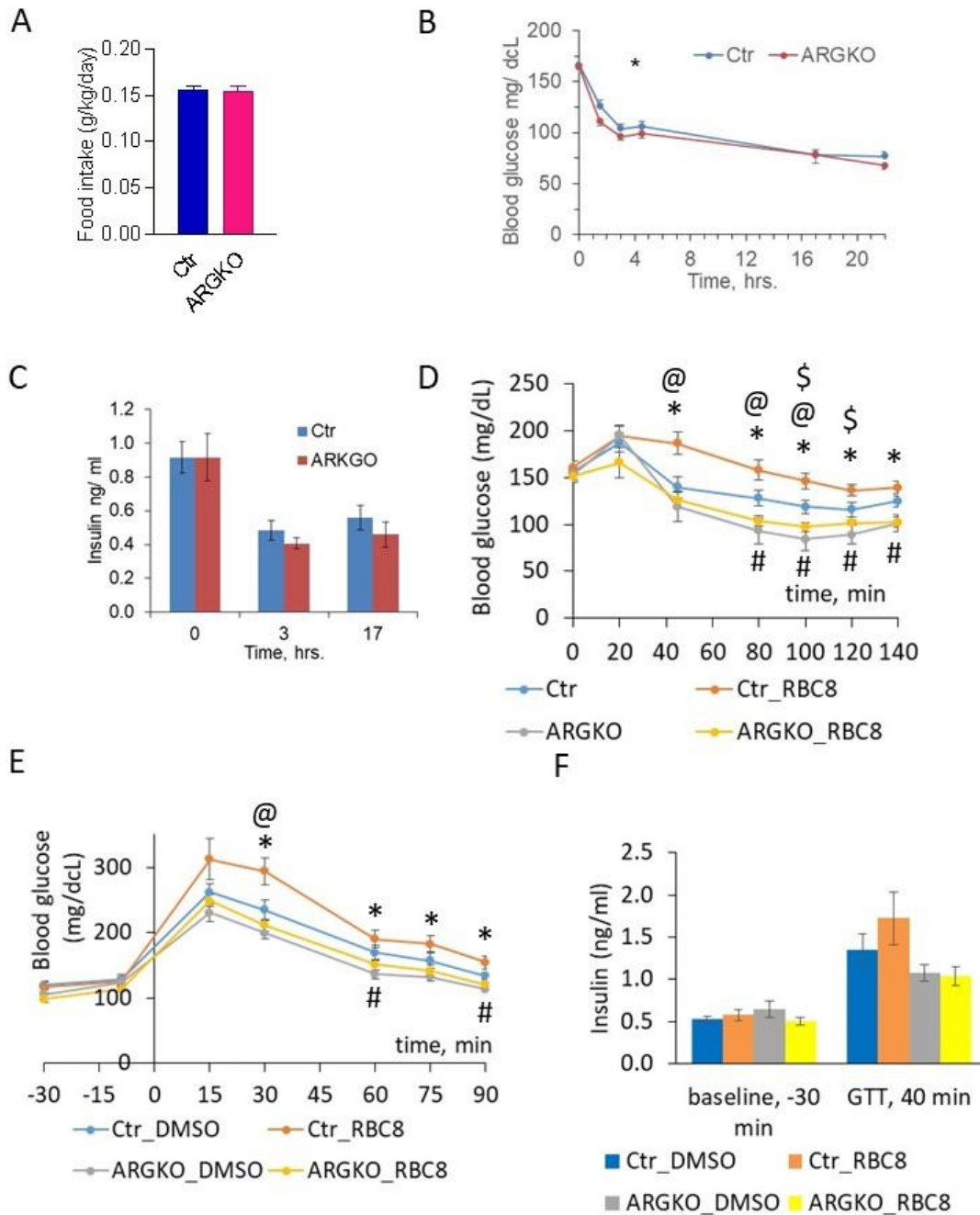


Fig. S7. Metabolic parameters in ARGKO mice on normal diet; RBC8 treatment.

A, food consumption, average over 7 days. *B,C*, Food was removed in the beginning of the night cycle. Blood glucose levels (*B*) and insulin (*C*) were measured before and after food removal. *D*, *Ad libitum* fed mice were injected with 50 mg/kg RBC8, then food was removed and blood glucose levels were measured. *E, F*, Mice were fasted for 6h, then injected with 50 mg/kg RBC8 (time point -20 min on the graph) and 20 min later (time point 0 min) injected with 1.2 mg/kg glucose. Blood glucose (*E*) and insulin levels (*F*) were measured during the experiment.

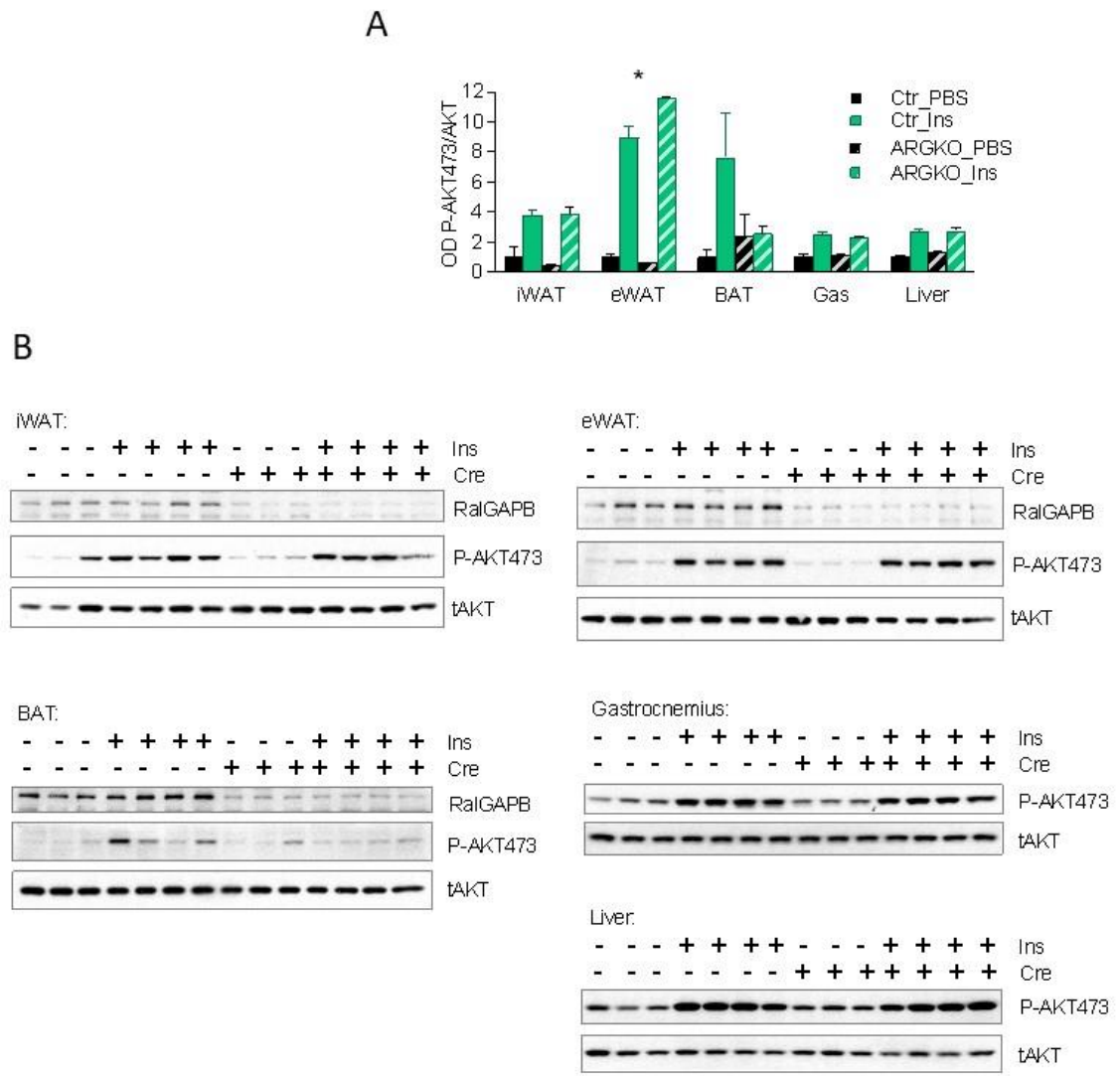


Fig. S8. Peripheral insulin sensitivity is not altered in ARGKO mice on normal diet. WB (B) and densitometry (A) of lysates collected after an overnight fast, with or without IP injection of insulin, 1U/kg. The data are presented as $Av \pm SEM$.

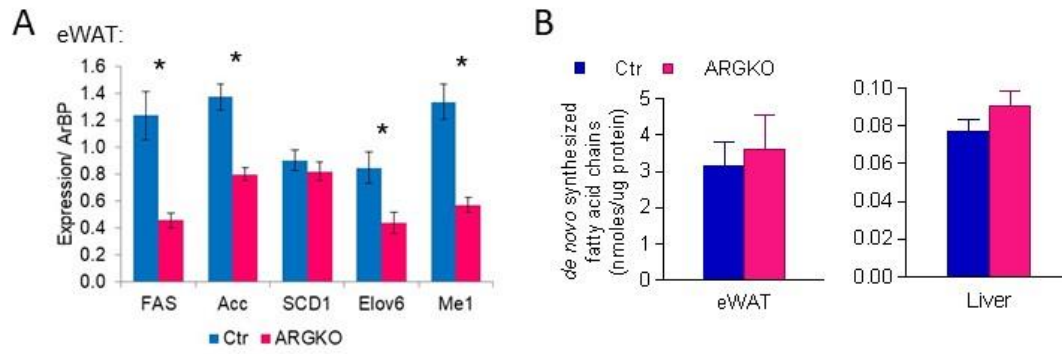


Fig. S9. *De novo* lipogenesis in ARGKO mice on normal diet.

A, Expression of *de novo* lipogenesis genes in eWAT. *B*, *DNL* in indicated tissues, was measured by mass spectrometry analysis of D2O incorporation into fatty acids.

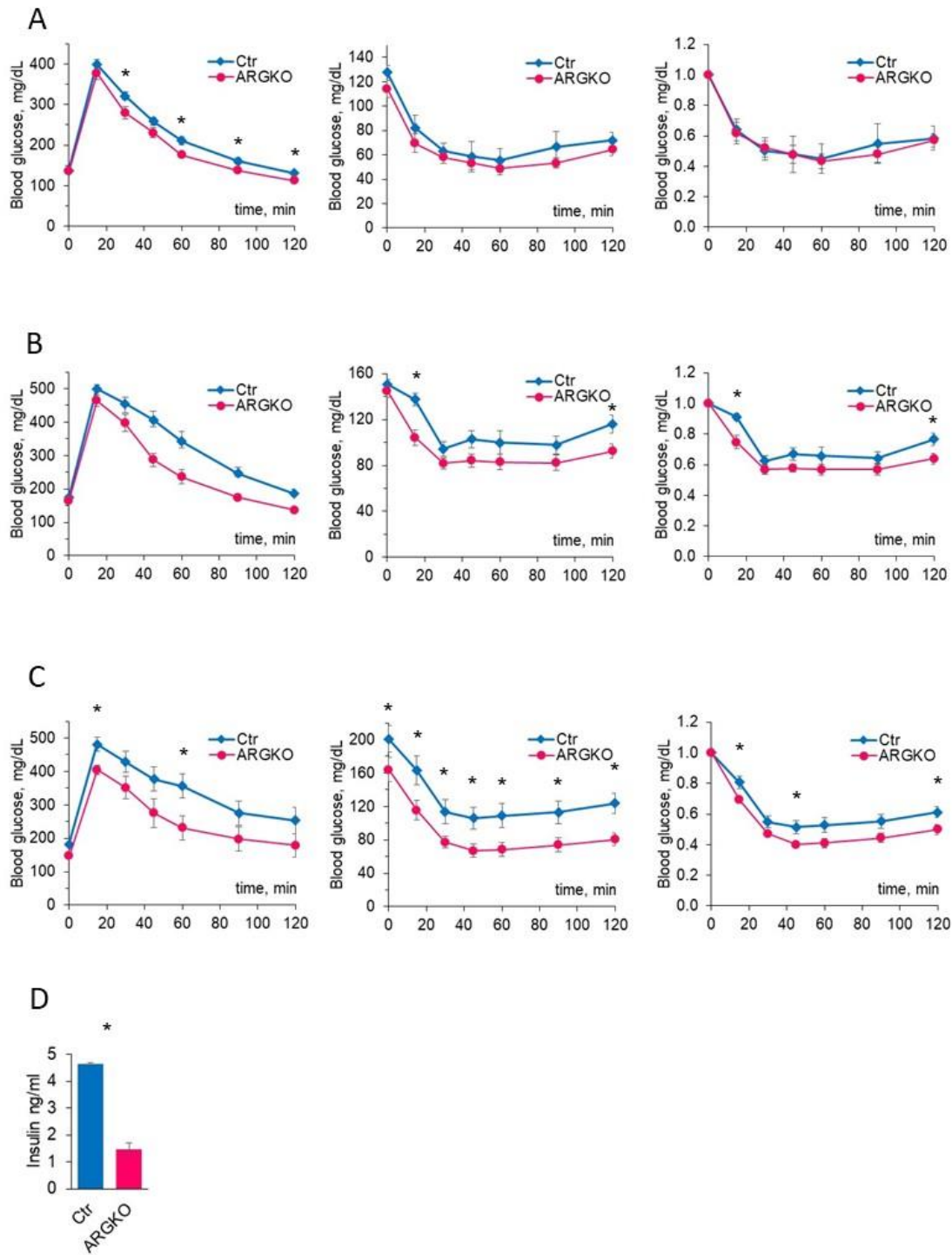


Fig. S10. Development of glucose and insulin intolerance is delayed in ARGKO mice on HFD.

A, GTT and ITT in 7 week old mice on normal diet chaw. B-C, Mice were placed on 45% HFD at 8 week age. GTT and ITT were performed after 3 (B), and 12 (C) weeks of HFD feeding. D, insulin at 12 weeks of HFD.

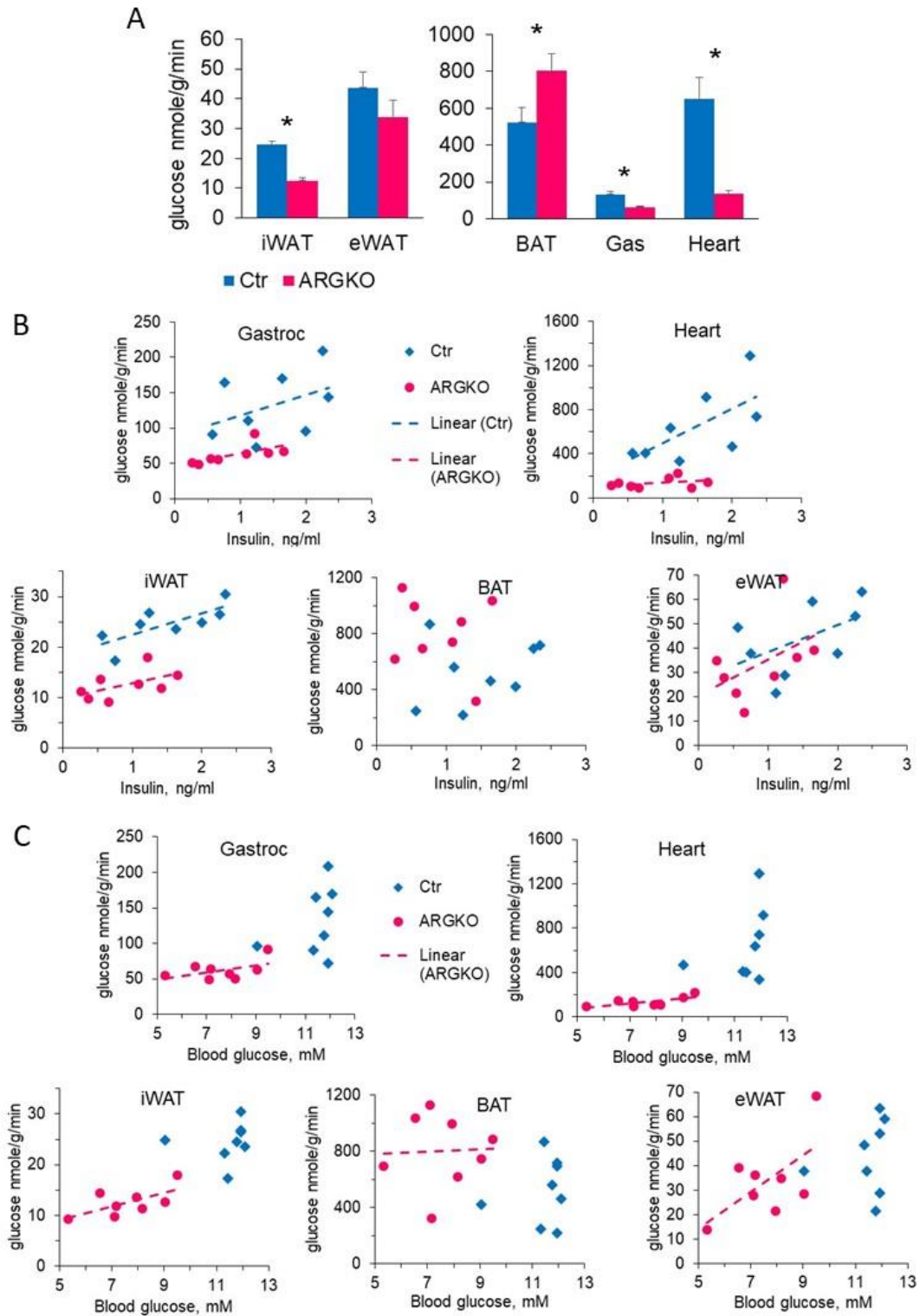


Fig. S11. *In vivo* glucose uptake in HFD-fed mice after 6hr fast.

A, Glucose uptake per g/tissue in HFD-fed mice after 6h fast. *B*, Glucose uptake per g of indicated tissue is plotted against plasma insulin concentration. *C*, Glucose uptake per g of indicated tissue is plotted against blood glucose levels.

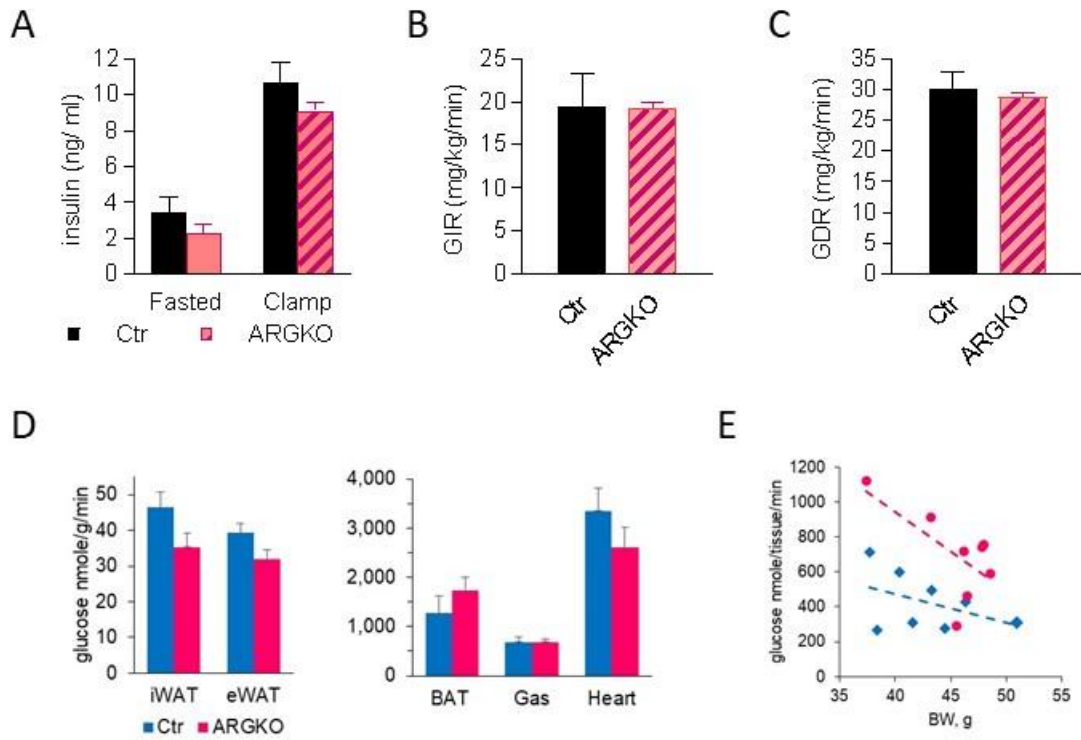


Fig. S12. Hyperinsulinemic-euglycemic clamp in ARGKO mice on HFD.
A, plasma insulin levels. *B*, glucose infusion rate. *C*, glucose disposal rate. *D*, tissue-specific glucose uptake during the clamp, presented per g of tissue. *E*, Glucose uptake per BAT during the clamp plotted vs. BW.

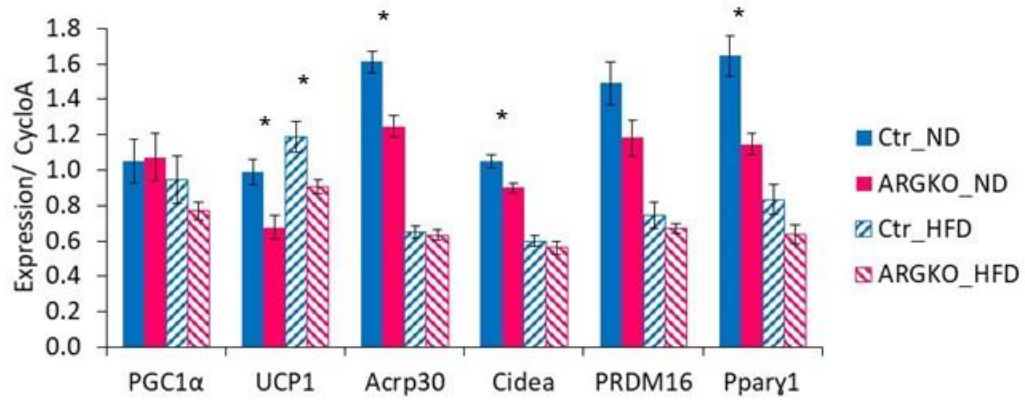


Fig. S13. Thermogenesis gene expression in BAT.

22 old mice on ND or mice that have been on HFD for 14 weeks, were fasted for 6hr and tissues were collected and processed for gene expression analysis.

Table S1. List of primers used for QPCR analysis.

Biological process	Gene name	F: 5'-3'	R: 5'-3'
Normalization	ArBP	CACTGGTCTAGGACCCGAGAA	AGGGGGAGATG TTCAGCATGT
	CycloA	GTG GTC TTT GGG AAG GTG AA	TTA CAG GAC ATT GCG AGC AG
Glucose Transporters	Slc2a4	GTGACTGGAACACTGGTCCTA	CCAGCCACGTTGCATTGTAG
	Slc2a1	CCTGTCTCTTCCTACCCAACC	GCAGGAGTGTCCGTGTCTTC
DNL	FASN	GGAGGTGGTGATAGCCGGTAT	TGGGTAATCCATAGAGCCCAG
	ACC1	TAA TGG GCT GCT TCT GTG ACT	CTC AAT ATC GCC ATC AGT CTT
	SCD1	GCT GGA GTA CGT CTG GAG	TCC CGA AGA GGC AGG TGT AG
		GAA	
	Elovl6	GAAAAGCAGTTCAACGAGAACG	AGATGCCGACCACCAAAGATA
	Me1	GTCGTGCATCTCTCACAGAAG	TGAGGGCAGTTGGTTTTATCTTT
SREBP1 α	CCGGGGAAC TTTTCCTTAAC	CAGGAAGGCTTCCAGAGAGG	
Thermogenesis	Ucp1	AGGCTTCCAGTACCATTAGGT	CTGAGTGAGGCAAAGCTGATTT
	Acrp30	TGTTCTCTTTATCCTGCCCA	CCAACCTGCACAAGTCCCTT
	Cidea	TGACATTCATGGGATTGCAGAC	GGCCAGTTGTGATGACTAAGAC
	Prdm16	CCACCAGACTTCGAGCTACG	ACACCTCTGTATCCGTCAGCA

References

1. Renner M, *et al.* (2010) Deleterious effects of amyloid beta oligomers acting as an extracellular scaffold for mGluR5. *Neuron* 66(5):739-754.
2. Lizunov VA, Stenkula K, Troy A, Cushman SW, & Zimmerberg J (2013) Insulin regulates Glut4 confinement in plasma membrane clusters in adipose cells. *PLoS One* 8(3):e57559.
3. Sbalzarini IF & Koumoutsakos P (2005) Feature point tracking and trajectory analysis for video imaging in cell biology. *J Struct Biol* 151(2):182-195.
4. Liu J, *et al.* (2005) Changes in integrin expression during adipocyte differentiation. *Cell Metab* 2(3):165-177.
5. Tsuboi KK & Petricciani JC (1975) Concentrative accumulation (active transport) of 2-deoxy-D-glucose in primate fibroblasts. *Biochem Biophys Res Commun* 62(3):587-593.
6. Guttman M, *et al.* (2009) Interactions of the NPXY microdomains of the low density lipoprotein receptor-related protein 1. *Proteomics* 9(22):5016-5028.